Dynamic Modeling and Simulation of Compressor Trains for an Air Separation Unit

S. Dominic *, **U. Maier** *

* *Institute of Automatic Control and Complex Systems (AKS),*
University of Duisburg-Essen, Bismarckstr. 81 BB, 47057 Duisburg,
Germany (e-mail: shane.dominic@uni-due.de)

Abstract: This paper presents dynamic models of a compressor train for an air separation unit. The model is derived from physical equations. A block library and complete models are implemented in Matlab/Simulink. Model accuracy is validated by comparing simulation results with realistic data gained from an existing industrial plant. The goal of modeling is to obtain a better understanding of the dynamic behavior in different operating modes and to get a base for design of new control strategies, *e.g.* a supervisory controller for minimizing power consumption of the total compressor train.

Keywords: Air Separation Unit; Compressor Modeling; Dynamic Simulation

1. INTRODUCTION

Cryogenic air separation units (ASU) are part of various industrial processes, *e.g.* in refinery, food, chemical or metallurgical industries. Depending on the process, the distillation unit produces high purity oxygen, argon or nitrogen. The process originally was developed by Carl von Linde in 1902. Important parts of an ASU are the compressors. They compress the filtered air from the environment to the necessary pressure. Afterwards the compressed air is cooled down to 100 K and separated into its three parts. Separation takes place in the distillation column. Due to the difference in boiling temperatures, the individual air components can be separated, each in liquid and gaseous form. This is purely a physical process. A detailed process description can be found in [Hands, 1986].

Nowadays, ASUs find new application in next generation fossil power plants, where CO_2 emission is to be reduced by using carbon capture and storage (CCS) methods. Some of the methods use oxygen instead of air for fuel combustion. This avoids N_2 and increases the CO_2 concentration in the flue gas and makes it easier to separate CO_2. CCS reduces CO_2 emissions by 90% or more, which would be an important contribution against global warming. Additional details for different CCS methods can be found in [Jansen, 2004].

The detailed structure of an ASU depends on the CCS process. Fig. 1 shows the ASU structure of interest, with two compressor stages, called main air compressor (MAC) and booster air compressor (BAC). Each of these stages contains more than one compressor, for example an axial and a radial compressor.

Integrating CCS with an ASU into a power plant will affect the efficiency of the plant, by reducing it up to 10%. [Bouillon et al., 2009] compare different solutions for a CCS power plant and conclude that an ASU is not suitable, because it would double the price of electricity.

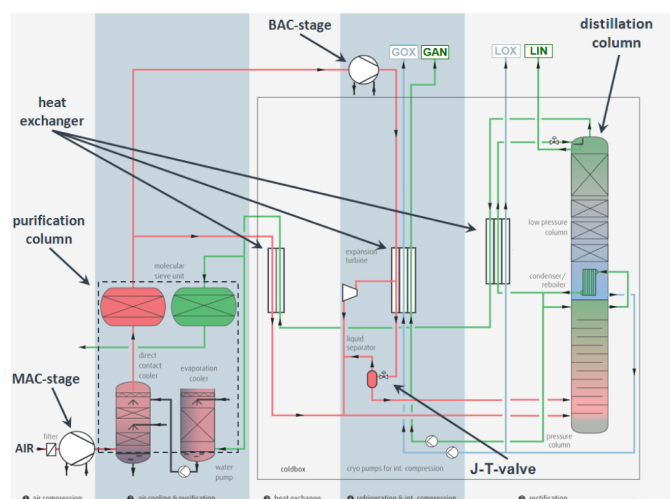To improve efficiency, new control approaches have been

Fig. 1. Typical structure of an ASU plant, [Linde, 2007]

studied, like dynamic optimization strategies using model predictive control [Zhu et al., 2011]. Zhu's paper presents an on-line optimization of the operating conditions of the ASU distillation part. A new high performance process controller (HPPC) has been introduced in [Vinson, 2006]. It requires that the control system operates the plant at optimal efficiency over the full range of steady-state and dynamic operating conditions. The ASU has to follow the changing operating points of the power plant. To optimize these dynamic changes, a homotopy-based backtracking method is applied in [Zhu et al., 2009]. Most publications have their main focus on the distillation column.

Until recently, there have been few studies of the compressor part, which can causes high power consumption. Instead of optimizing the existing basic machine controllers and the individual components, the idea is to design a new supervisory controller for the whole compressor train, which not has been done until now.

Depending on the plant configuration, there are more

actuating signals than controlled variables. Thus, for each operating point of the power plant, the required operating conditions for the compressors can be reached by different set point combinations for the underlying basic machine controllers. This degree of freedom can be used for optimization, *i.e.* power minimization.

For design of the new optimizing controller, models of the ASU are required. Especially, a better understanding of compressor train dynamics is required by running simulations.

Section 2 outlines the derivation of the physical equations in order to build the model. Section 3 presents simulation results. Section 4 compares simulation results with measurement data from an existing industrial plant, in order to validate the models. The final section 5 contains conclusions.

2. ASU MODELING

For building the dynamic ASU models, the toolkit MATLAB/Simulink is used. The aim is to create a library with new blocks for each element of the compressor train like pipes, compressors, valves and coolers. An additional objective is adaptability for other processes like fuel gas compression or chemical production of nitric acid (HNO_3). Most of the ASU plants are powered by a steam turbines. Since models of steam turbine are readily available, this component will not be considered in this paper. Instead, models for the remaining components will be developed. In the following, the required physical equations for the mentioned elements are derived.

2.1 Pipe Model

The units of an ASU plant are interconnected by pipes with flowing air. The model equations can be gained from thermodynamics and fluid dynamics. The three basic equations are

- thermic state equation of gas,
- continuity equation,
- motion equation.

It is assumed that the cylindrical pipe lengths are much larger than their diameter, and that the flow can be regarded as a one-dimensional flow string. The pipes are fixed in space and are assumed to have no elastic deformation. The thermic state equation of a gas is

$$p = \rho \cdot R \cdot T \cdot z, \quad (1)$$

with pressure p, density ρ, specific gas constant R, temperature T, and real gas factor z. The mass flow $\dot{m}$ through a pipe cross section area A with velocity w is

$$\dot{m} = \rho \cdot A \cdot w. \quad (2)$$

The mass dm in a pipe piece of length dx is

$$dm = \rho \cdot A \cdot dx. \quad (3)$$

The change of dm with time depends on the difference between inlet and outlet flow, *i.e.*

$$\frac{\partial(dm)}{\partial t} = \dot{m} - [\dot{m} + \frac{\partial \dot{m}}{\partial x} dx] = -\frac{\partial \dot{m}}{\partial x} dx. \quad (4)$$

Applying (3) into (4) yields

$$\frac{\partial(\rho A dx)}{\partial t} = -\frac{\partial \dot{m}}{\partial x} dx. \quad (5)$$

or

$$\frac{\partial \rho}{\partial t} = -\frac{1}{A} \cdot \frac{\partial \dot{m}}{\partial x}. \quad (6)$$

Another assumption is that energy losses by heat transfer, wall friction or turbulences can be neglected, such that we can assume an isentropic flow, *i.e.* [Maier, 2008]

$$\frac{p}{\rho^\kappa} = const = c, \quad (7)$$

where with (1) the constant c is

$$c = \frac{p}{\rho^\kappa} = \frac{p}{\rho^{\kappa-1}\rho} = \frac{RTz}{\rho^{\kappa-1}} \quad (8)$$

By differentiating (7) and applying (8) and (6) we get

$$\frac{\partial p}{\partial t} = -\frac{\kappa RTz}{A} \cdot \frac{\partial \dot{m}}{\partial x}. \quad (9)$$

To derive the motion equation, we use the force balance in the considered pipe element, yielding

$$dm \cdot \frac{dw}{dt} - pA + pA - \frac{\partial}{\partial x}(pA) \cdot dx + F_R \cdot dx = 0. \quad (10)$$

where F_R means the wall friction force per pipe length. It can be described by

$$F_R = \frac{\lambda RTz}{2DA} \cdot \frac{\dot{m}^2}{p}. \quad (11)$$

The constant λ is the friction factor, which depends on the Reynolds number and the pipe wall surface roughness. With the derivation of the velocity w over time

$$\frac{dw}{dt} = \frac{\partial w}{\partial t} + w \cdot \frac{\partial w}{\partial x}, \quad (12)$$

the formula for force balance and the continuity equation we get the motion equation

$$\frac{\partial \dot{m}}{\partial t} = \frac{2\dot{m}}{\rho \kappa RTz} \cdot \frac{\partial p}{\partial t} + [\frac{2\dot{m}^2}{\rho^2 A\kappa RTz} + A] \cdot \frac{\partial p}{\partial x} - F_R. \quad (13)$$

Integrating the continuity equation and the equation of motion along the pipe length, yields the following two equations, which we can use for the modeling

$$\frac{dp_{in}}{dt} = \frac{\kappa RzT_{in}}{AL} \cdot [\dot{m}_{in} - \dot{m}_{out}], \quad (14)$$

and

$$\frac{d\dot{m}_{in}}{dt} = \frac{2\dot{m}_{in}}{\rho \kappa RTz} \cdot \frac{dp_{in}}{dt} + [\frac{2\dot{m}_{in}^2}{\rho^2 A\kappa RTz} + A]\frac{p_{in} - p_{out}}{L} - F_R. \quad (15)$$

The entire derivation is explained in [Blotenberg, 1988]. The two following terms in equation (13) can be neglected without losing the accuracy of the result [Gronau, 1983]

$$\frac{2\dot{m}_{in}}{\rho \kappa RTz} \cdot \frac{dp_{in}}{dt}, \quad (16)$$

and

$$[\frac{2\dot{m}_{in}^2}{\rho^2 A\kappa RTz}] \cdot \frac{p_{in} - p_{out}}{L}. \quad (17)$$

Hence it is assumed that there is no heat transfer in the pipe, consequently the inlet and outlet temperature are the same. But for mixing junctions with more than one

incoming mass flow and different temperature of the flows the outlet temperature has to be calculated. Using the enthalpy balance, the continuity and the gas equation, outlet temperature can be calculated as follows

$$\frac{d\dot{T}_{out}}{dt} = \frac{T_{out}}{p_{out}} \cdot [\frac{dp_{out}}{dt} - (\dot{m}_{in} - \dot{m}_{out})\frac{Rz}{AL} \cdot T_{out}]. \quad (18)$$

With these equations the general pipe block can be build. The specific parameters of the block are pipe diameter, length and the friction factor.

2.2 Compressor model

Modeling of the compressors is the core piece of the ASU model. In order to describe the dynamic behavior of the machines as precisely as possible, the characteristic map of the machine is used. In this map, shown in fig. 2, the enthalpy difference is a function of the volume flow, the inlet guide vane (IGV) position, or the rotational speed. In case of constant IGV position, the volume flow will only change along the corresponding IGV curve. Depending on the type of control, IGV position or speed, the map contains lines for the the constant IGV or constant speed. There is also a surge line in the map. This line separates the map into stable and unstable working points. Here, unstable means that the machine begins to "surge" or "pump", *i.e.* the fluid periodically flows back from the pressure side to the suction side and this can cause significant machine damage [Bogatzki, 2010]. To prevent this, each compressor is equipped with an anti surge controller (ASC). As soon as the working point passes the control line, the controller will open the valves to increase the volume flow. Consequently the working point will move to the right side and the compressor restabilises.

The specific enthalpy is a state variable, that characterizes the total energy of a system, which depends on the internal energy of the system, the pressure and volume [Stephan et al., 2006]. The specific enthalpy difference $\triangle h$ can be expressed by the pressure ratio and the isentropic exponent κ [Meny, 2006],

$$\triangle h = (\frac{1}{\kappa - 1} + z) \cdot R \cdot T_{in} \cdot [(\frac{p_{out}}{p_{in}})^{\frac{\kappa-1}{\kappa}} - 1]. \quad (19)$$

This equation can be used with the assumption for ideal gas

$$c_v = \frac{f}{2} \cdot R. \quad (20)$$

c_v is the specific heat capacity and f is the degree of freedom.

There are two ways to determine the volume flow. For both, the enthalpy difference is needed. One method is using the compressor map, fig. 2. According to the enthalpy difference and the IGV position or the rotation speed, the volume flow can be found. The curves also can be described by polynomials. The second method is to calculate the volume flow by using a mathematical equation. This contents the geometrical parameters of the compressor, which was not available for our studies. Since the compression of a fluid is not an isothermal process, the outlet temperature has to be also calculated here. The outlet temperature depends mainly on the isentropic efficiency η_s of the machine and the pressure difference.
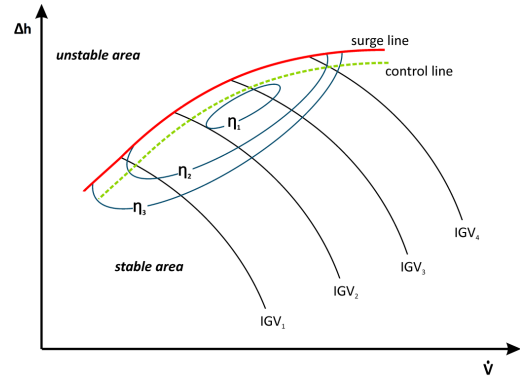

Fig. 2. Compressor map for an IGV controlled machine

The mathematical description can be written as [Blotenberg, 1988]

$$T_{out} = \frac{1}{\eta_s} \cdot T_{in}[(\frac{p_{out}}{p_{in}})^{\frac{\kappa-1}{\kappa}} - 1] + T_{in}. \quad (21)$$

In order to calculate the power of the compressor, the process is considered as an adiabatic compression, which implies that we can neglect the thermal loss, since the supplied energy to the fluid is much larger. The power for the compressor to lift the mass flow $\dot{m}$ is [Stephan et al., 2006]

$$P = \frac{\dot{m}_{in} \cdot \triangle h}{\eta_s}. \quad (22)$$

By using the isentropic efficiency η_s of the machine the friction is considered Due to the complexity of the calculation, we estimate the isentropic efficiency from the efficiency curves of the compressor map, blue curves in fig. 2. By using these equations the compressor can be described very well.

2.3 Valve Model

A further required element is the valve block. Valves play an important role in protecting the compressors. When the compressor becomes unstable and begins to surge (pump), the ASC will open valves to increase the flow rate in the compressor, which brings it to a stable point. There are two possible types of protection valves: a blow-off valve, which releases the compressed fluid into the environment; and a recycle valve, which leads the flow back to the compressor suction side. The opening and closing time of the valves should be modeled carefully in order to correctly describe the dynamic behaviour when crossing the control line. Then, the simulations can help to choose suitable valves. These time parameters are one of the specific parameters of the developed Simulink valve block.

In addition to the surge protection valves, fig. 1 also shows that there is a Joule-Thomson valve in an ASU. The purpose of this valve is to control the discharge pressure of the BAC stage. The volume flow through the valve depends on the flow coefficient and on the pressure ratio. The flow coefficient K_V mainly depends on the valve position. For this dependency, there exist different characteristics: linear or equal percentage. There are two different cases for the volume flow calculation, a subcritical or a supercritical pressure ratio. Subcritical means, the outlet pressure is more than about half the

inlet pressure. Supercritical is the opposite of subcritical. There is a specification for the flow calculation, DIN IEC 60534 [Kollar, 2000]. According to the pressure ratio there are different mathematical description for the calculation of volume flow, which mainly depends on the following values

$$\dot{V}_{in} = f(K_V, \triangle p, \rho_n, T_{in}). \quad (23)$$

ρ_n is the standard density for the pressure 1 bar and for the temperature 273.15 K. The outlet pressure can be calculated with the equation

$$\frac{\partial p}{\partial t} = \frac{\kappa R T z}{V} \cdot \frac{\partial \dot{m}}{\partial t}. \quad (24)$$

Here V is the volume of the valve.

2.4 Cooler and Heat Exchanger Model

Heat exchangers are essential components of the ASU plant. Since the focus of modeling is the compressor train, exact modeling is not required. Since the outlet temperature is known, Heat exchangers are simulated like pipes with the required outlet temperature. Condensation of the water vapor inside the cooler is taken into account. The condensation is important, because the air is dried after the MAC stage. That means, the volume flow will be reduced by the content of water vapor. Another reason to consider the water vapor content is that the gas constant R depends on it. According to the relative humidity, the water content can be determined from the saturation curve. This curve characterizes the maximum water content depending on the temperature. The current content of the water can be defined by the humidity. If it is higher than the allowed water content, the difference has to be subtracted, because it condensates and is removed. The humidity can be recalculated with the new concentration of water vapor.

3. SIMULATION RESULTS

Using the equations from section 2, we developed a simulation platform with a particular library. For each plant component like compressor or pipe, a block type has been developed. Fig. 3 shows as an example the model of a compressor train for an ASU plant. The structure looks similar to the ASU scheme in fig. 1. In section 2, modeling of the purification and distillation column was not presented. Exact modeling of these parts might be too complex and is not needed for our purposes. Therefore these parts are considered as pipes with the specific geometrical properties and the desired outputs. Using these models, the following operating modes can be analyzed:

- startup performance,
- shutdown behavior,
- performance on the control line and pressure limiting curve.

Most of the working points are close to the control line. To test undelayed shutdowns, the volume flow is suddenly decreased, while the pressure ratio remains almost constant. This could cause a movement of the working point into the unstable area. Undelayed shutdown means, that the steam turbine is shut down and blow-off valves are opened instantly at the same time. Another critical situation is
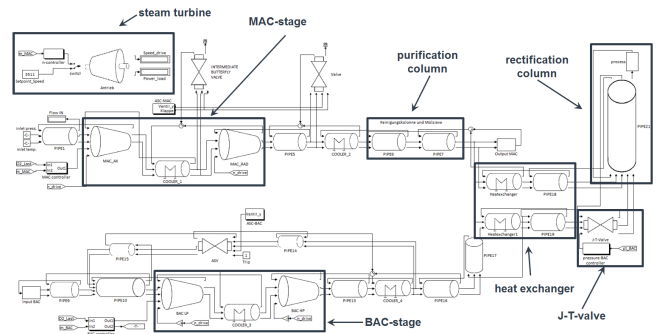

Fig. 3. Model implementation with Matlab/Simulink

the behavior on the pressure limiting curve. When the process flow resistance increases, the pressure ratio of the compressor gets higher, which could also lead to instability. To avoid the unstable working points, the opening time T_{on} and the flow coefficient K_v of the blow-off and recycle valves have been adapted to the compressor size and the volume flow.

In most cases the industrial plants need more than one compressor train. To keep cost low, the valve sizes should be as small as possible. One compressor train needs at least 5 valves. Therefore minimizing the valve size, will reduce cost by several thousand euros.

The startup procedure is less critical. The working point will move along the process resistance curve. However a future requirement will be an improved performance, *i.e.* faster and less energy consumption.

The library also includes the actual ASC controllers with the authentic parameter settings.

Therefore, this new simulation toolbox facilitates the investigation of the performance and stability of the compressor train. Furthermore the robustness of the machine at the design points during faults also can be analyzed.

Preliminary results are presented based on simulations from different operating modes. Due to the confidentiality agreement with the industrial partners, only the MAC stage will be presented here. Validation of the results will be given in Section 4.

3.1 Shutdown Simulation

When the plant is shut down, the blow valves are opened and the steam turbine slows its rotation speed down to zero after some time. In this case the volume flow decreases and falls along the process resistance line. This is called a delayed trip, as it is shown in fig. 4 (blue curve).

In this figure, the IGV controlled compressor map of the MAC stage is depicted. In this case the compressor does not get unstable. Except in the case of an undelayed trip, the valves are opened instantly. This causes a movement of the working point almost parallel to the flow axis.

If the K_V value is too small or the opening time too large, the pressure ratio of the compressor would not decrease fast enough and the compressor will become unstable.

To overcome this problem, the valve properties should be adjusted. The magenta curve in fig. 4 indicates the behavior of the undelayed trip with suitable valve properties and the magenta dashed line with unsuitable valve properties. The simulation results give a good suggestion of which valves are best suited for this type of compressor train.
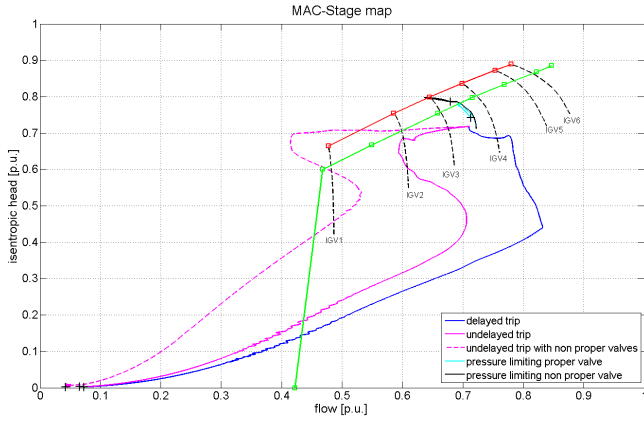
Fig. 4. Simulation results shown as a compressor map

Figure 5 shows the time behavior of rotation speed, the position of a blow-off valve, the overall output pressure of the MAC stage and the axial part of MAC. Also the volume flow is shown.

In the delayed trip case, the valves are opened after 3 seconds and for the undelayed one they were opened directly. The figure clearly shows the difference between the delayed and the undelayed trip. Especially the different behavior of a different valve size can be seen here, by comparing the magenta and the magenta dashed curve. The MAC pressure output is almost constant at the beginning and therefore the machine becomes unstable.

3.2 Pressure Limitation Simulation

In some cases it happens, that the process-resistance of the plant changes unexpectedly, caused by some disturbances or faults. As a consequence the pressure ratio of the compressor will change. As mentioned above, an increase of the pressure ratio will move the working point nearly parallel to the y-axis into the instability area. To avoid this, the ASC controller opens the blow-off valves. Using wrong valve sizes will move the working point into the unstable area for a short time, as it is shown in fig. 4 (purple curve). However, with suitably-sized valves, the working point will not cross the control line (cyan curve).
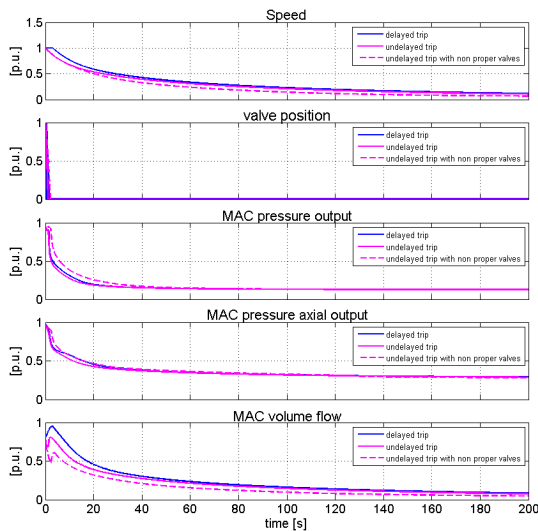

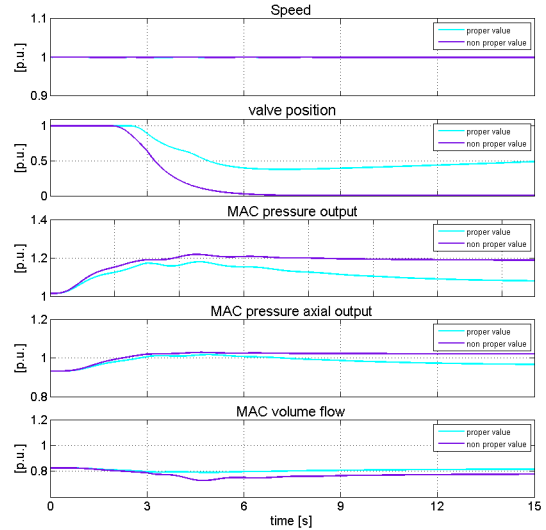Fig. 5. Shutdown simulation results as a function of time

Fig. 6. Pressure limitation simulation results as a function of time

The cross marks the final working point at the end of simulation.

For the non-suitable valve case, the ASC controller has to open the valve totally in order to reduce the MAC pressure output, as it is depicted in subplot 2 in fig. 6 (violet curve). But in the other case it is not necessary to open the blow-off valve totally, because the working point could be regulated at the control line (cyan curve).

4. MODEL VERIFICATION

Model validation is done by comparing simulation results with measurement data of an existing industrial plant. The structure of the existing plant is similar to the structure shown in fig. 3.

One example is presented here. Fig. 7 shows an undelayed trip situation after 24 seconds with the time behavior of rotation speed, valve position of a blow-off valve, the MAC overall pressure output and the axial part of MAC. Also the MAC volume flow is shown here. The blue curves show the measurement data and the red ones the simulation results. There is a good match for the compressor speed and the valve position. This indicates that the model simulates the dynamic behavior correctly.

Comparing pressures, we can see that the static behavior matches, but the dynamic behavior shows some deviations. The simulated pressure falls off a little bit faster than the measured pressure. After analyzing more measurement data, we could conclude that a possible cause is the slow response of the pressure transmitter. To compensate the deviation, we try to simulate the lag of the transmitter with a first order lag block. The red dashed lines in subplots 3 and 4 show the new simulation results. As it can be seen, the deviations are much smaller. Also the gradual reduction of the MAC axial pressure, as it can be seen in subplot 4, is caused by the pressure transmitter.

For the MAC pressure output, there are two measurement data available from two different sensors. One of them shows the same gradual reduction behavior. Therefore we conclude that the transmitter affects the data.

Table 1 shows the mean squared error (MSE) between the simulation result and the measurement data. It is divided

into two part, static point and the undelayed trip part. The variance in the static part is negligible. For the second part, the largest value is 1.7e-3. This is in a tolerable range. The correlation between the simulation results with the developed models and the measurements is good. The static behavior is modeled very well. This also is true for the dynamic behavior, only with some minor exceptions. The steam turbine and the valves are modeled almost exactly. The dynamic behavior of the pressure and the volume flow are modeled quite well and are improved by using a first order lag to describe the pressure transmitter. In some validation tests of shutdown processes the simulation results show that the compressor stages run stable. While the measurements indicate, that the machines became unstable. Further investigations revealed, that the blow off valves couldn't open as fast as they should, due to the slow mechanical valve control. Replacing it by electrical valve control, the desired opening and closing time can be achieved. Thus, the stability can be ensured, like it is shown in the simulation results. Also the results for other operating modes like start ups are proved to have the same accuracy.

5. CONCLUSION AND FUTURE WORK

This paper presents the results of dynamic modeling of an ASU plant, which is described by the physical equations from thermodynamics and fluid mechanics. This model is compared with real plant data from an existing industrial ASU plant. It was shown that the developed model was able to simulate correctly both the dynamic and the static regions of the system.

Based on an analysis of this model, the start up, shut down and along the control line modes of operation can be analyzed more efficiently. The simulation model helps, to investigate the stability for critical operating modes. Another important point is, that this simulation toolbox provides new opportunity to examine the existing control loops and to improve them. The next step is to find new control strategies for the operating modes, in order to reduce the energy consumption
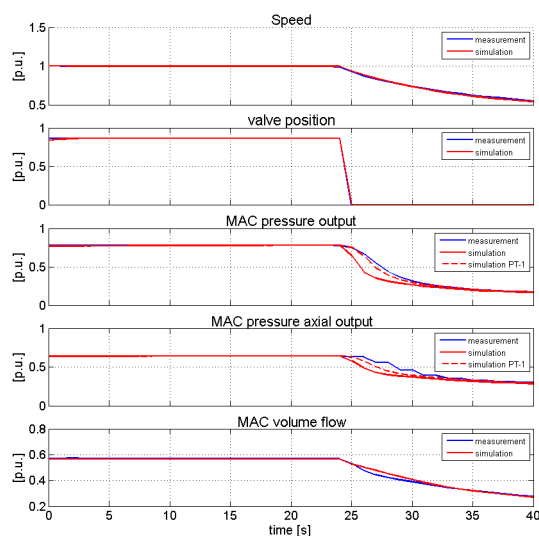

Fig. 7. Model validation
    blue: measurement data, red: simulation results

variable	static point MSE/[p.u.]	undelayed trip MSE/[p.u.]
rotation speed	1.47e-5	1.13e-5
valve position	3.65e-5	2.90e-5
press. out. MAC	2.62e-5	8.40e-3
press. out. MAC (PT1)	3.20e-5	5.53e-4
press. out. MAC-Ax	3.44e-6	5.30e-3
press. out. MAC-Ax (PT1)	3.82e-6	1.70e-3
volume flow MAC	2.44e-5	2.43e-4

Table 1. MSE values

during the stationary operation. The simulation model shows, that different set point combinations lead to different energy consumption. Based on this new knowledge the supervisory controller will be designed to achieve the most efficient operating mode. Due to the space limitation the results of this study will be presented in different paper.

REFERENCES

W. Blotenberg. *Ein Beitrag zur digitalen Pumpschutzregelung von Turbokompressoren.* PhD thesis, University Bochum, 1988.

D. Bogatzki. Entwicklung und SPS-Implementierung eines Algorithmus zur Zustandsberwachung von Kompressoren. Master thesis, University Duisburg-Essen, 2010.

P.A. Bouillon, S. Hennes, and C. Mahieux. ECO2: post-combustion or Oxyfuel comparison between coal power plants with integrated CO2 capture. *Energy Procedia*, pages 4015–4022, February 2009.

M. Gronau. Ein Beitrag zur theoretischen Modellbildung von Verdichteranlagen. Schriftreihe Heft 19, Mess- und Regelungstechnik der Universitaet Bochum, 1983.

B. A. Hands, editor. *Cryogenic engineering.* Academic Press, London ; Orlando, 1986.

D. Jansen. Technologies and Possibilities for CO_2 Capture and Storage. In *International Conference on Innovation and Future Developments in Cement Production concrete Constructions*, 2004.

L. Kollar. *Automatisierungstechnik 3* , chapter Bemessungsgleichungen fuer Stellglieder nach DIN/IEC 534, pages 67–84. Springer Verlag, Berlin Heidelberg, 2000.

Linde. Cryogenic air separation, history and technological progess, 2007.

U. Maier. Modelling and Simulation of Dynamic Systems, 2008. Lecture notes, University Duisburg-Essen.

K. Meny, editor. *Stroemungsmaschinen, Hydraulische und thermische Kraft- und Arbeitsmaschinen.* Teubner Verlag, Wiesbaden, 2006.

P. Stephan, K. Schaber, K. Stephan, and F. Mayinger, editors. *Thermodynamik, Grundlagen und technische Anwendungen, Band 1: Einstoffsysteme.* Springer Verlag, Berlin Heidelberg, 2006.

David R. Vinson. Air separation control technology. *Computers & Chemical Engineering*, pages 1436–1446, 2006.

Lingyu Zhu, Zhiqiang Chen, Xi Chen, Zhijiang Shao, and Jixin Qian. Simulation and optimization of cryogenic air separation units using a homotopy-based backtracking method. *Separation and Purification Technology*, pages 262–270, 2009.

Y. Zhu, S. Legg, and C.D. Laird. Optimal operation of cryogenic air separation systems with demand uncertainty and contractual obligations. *Chemical Engineering Science*, 66:953–963, March 2011.